Earth and Planetary Science Letters 426 (2015) 216–224

Contents lists available at ScienceDirect

Earth and Planetary Science Letters

www.elsevier.com/locate/epsl

First-principles investigation of vanadium isotope fractionation in solution and during adsorption

Fei Wu [a,*], Tian Qin [b,c,*,1], Xuefang Li [d], Yun Liu [d], Jen-How Huang [e], Zhongqing Wu [b,c], Fang Huang [a]

[a] CAS Key Laboratory of Crust-Mantle Materials and Environments, School of Earth and Space Sciences, University of Science and Technology of China, Hefei 230026, Anhui, China
[b] Laboratory of Seismology and Physics of Earth's Interior, School of Earth and Space Sciences, University of Science and Technology of China, Hefei, Anhui 230026, China
[c] Mengcheng National Geophysical Observatory, School of Earth and Space Science, University of Science and Technology of China, Hefei, Anhui, 230026, China
[d] State Key Laboratory of Ore Deposit Geochemistry, Institute of Geochemistry, Chinese Academy of Sciences, Guiyang 550002, China
[e] Environmental Geosciences, University of Basel, CH-4056 Basel, Switzerland

ARTICLE INFO

Article history:
Received 1 February 2015
Received in revised form 4 June 2015
Accepted 24 June 2015
Available online 10 July 2015
Editor: D. Vance

Keywords:
vanadium isotope
equilibrium isotope fractionation
density functional theory
redox
adsorption

ABSTRACT

Equilibrium fractionation factors of vanadium (V) isotopes among tri- (V(III)), tetra- (V(IV)) and penta-valent (V(V)) inorganic V species in aqueous system and during adsorption of V(V) to goethite are estimated using first-principles calculation. Our results highlight the dependence of V isotope fractionation on valence states and the chemical binding environment. The heavy V isotope (^{51}V) is enriched in the main V species following a sequence of V(III) < V(IV) < V(V). According to our calculations, at 25 °C, the equilibrium isotope fractionation factor between $[V^{5+}O_2(OH)_2]^-$ and $[V^{4+}O(H_2O)_5]^{2+}$ ($\ln\alpha_{V(V)-V(IV)}$) is 3.9‰, and the equilibrium isotope fractionation factor between $[V^{5+}O_2(OH)_2]^-$ and $[V^{3+}(OH)_3(H_2O)_3]$ ($\ln\alpha_{V(V)-V(III)}$) is 6.4‰. In addition, isotope fractionation between +5 valence species $[V^{5+}O_2(OH)_2]^-$ and $[V^{5+}O_2(H_2O)_4]^+$ is 1.5‰ at 25 °C, which is caused by their different bond lengths and coordination numbers (CN). Theoretical calculations also show that light V isotope (^{50}V) is preferentially adsorbed on the surface of goethite. Our work reveals that V isotopes can be significantly fractionated in the Earth's surface environments due to redox reaction and mineral adsorption, indicating that V isotope data can be used to monitor toxic V(V) attenuation processes through reduction or adsorption in natural water systems. In addition, a simple mass balance model suggests that V isotope composition of seawater might vary with change of ambient oxygen levels. Thus our theoretical investigations imply a promising future for V isotopes as a potential new paleo-redox tracer.

1. Introduction

Vanadium (V) is a redox sensitive element that has been widely used to constrain variation of redox conditions during many geological processes, including core-mantle segregation (e.g., Siebert et al., 2013), mantle evolution and melting (e.g., Lee et al., 2005), and low temperature processes on the Earth's surface (e.g., Breit and Wanty, 1991). Especially as V has multiple valances in seawater, it can be used as a redox tracer to study paleo-environment and paleo-oceanography (e.g., Algeo and Maynard, 2004). As a conservative or near conservative element with a residence time of ~100,000 years in seawater (about 20 times longer than the seawater cycle) (Morford and Emerson, 1999), V is nearly uniformly distributed in the ocean. Therefore, understanding transportation and removal of V in the seawater and precipitation of V into marine sediments has global implications. Furthermore, industrial exploitation of V could result in environmental problems as V is toxic to plants, animals, and human bodies (e.g., McCrindle et al., 2001). For regulation and evaluation of potential V pollution, it is important to identify the source and monitor V transportation and attenuation in solution.

An understanding the chemical behavior of V in water is important to understand the cycling of V in surface environments. V undergoes very complex hydrolysis in solution, where

* Co-first author, corresponding author. Tel.: +86 13225691203 (F. Wu) or +1 6129136866 (T. Qin).
E-mail addresses: fey@mail.ustc.edu.cn (F. Wu), tianqin91@gmail.com (T. Qin).
[1] Present address: Department of Earth Sciences, University of Minnesota, Minneapolis, MN 55455, USA.

http://dx.doi.org/10.1016/j.epsl.2015.06.048
0012-821X/

the species of V in solution are controlled by pH, Eh, concentration and aquatic chemistry. Fig. 1 shows the Eh–pH diagram for V aqueous in dilute V solutions ($[V]_{total} < 10^{-4}$ mol/L), which applies to most natural water including seawater and freshwater. In oxidizing conditions, V is mainly presented as V(V) in the form of vanadate oxyanion (HVO_4^{2-} and $H_2VO_4^-$) in natural water. At environmentally-impacted sites, which are typically associated with mining activities, V(V) could also form polynuclear species such as decavanadate ($H_xV_{10}O_{28}^{x-6}$) or metavanadate ($(VO_3)_x^{x-}$) at high concentrations. V(V) is highly soluble and mobile, and is the most toxic form of V in solution. Meanwhile, adsorption of V(V) onto iron and manganese oxides or clay minerals is one of the main controls of V concentration in modern seawater (Trefry and Metz, 1989; Elderfield and Schultz, 1996), river water (Auger et al., 1999), and groundwater (e.g., Breit, 1995). Under mildly or strongly reducing conditions, dissolved V(V) tends to be reduced to V(IV) or further to V(III) by organic compounds or H_2S (Breit and Wanty, 1991; Wanty and Goldhaber, 1992). V(IV) species are less soluble than V(V) and thus are apt to coprecipitate with minerals and organic substances (Breit and Wanty, 1991; Morford and Emerson, 1999), while V(III) species are insoluble and tend to precipitate from natural water as solid oxide or hydroxide (Wehrli and Stumm, 1989). Therefore, transportation and segregation of V in solution is mainly controlled by redox state variation and mineral adsorption–desorption.

V has two stable isotopes, ^{50}V (0.24%) and ^{51}V (99.76%). Highly precise and accurate V isotope data have recently been obtained due to the advancement of instruments (MC-ICP-MS) and chemical purification techniques (0.12–0.15‰, 2SD, Prytulak et al., 2011; Nielsen et al., 2011). V isotope data are expressed as: $\delta^{51}V = [(^{51}V/^{50}V)_{sample}/(^{51}V/^{50}V)_{reference} - 1] \times 1000$. Studies on mantle xenoliths and mafic lavas gave an estimation of the V isotopic composition of bulk silicate earth, and showed that V isotope can be fractionated during high-temperature magmatic processes such as mantle melting and mineral fractional crystallization (Prytulak et al., 2013). V isotope measurement of meteorites indicates that the silicate Earth is enriched in ^{51}V by about 0.8‰ relative to chondrites, likely reflecting the different irradiation history of the solar system (Nielsen et al., 2014).

Theoretical investigation and experimental work has shown that isotopes of multi-valence elements (e.g., Cr and Fe) can be fractionated during redox reactions (e.g., Anbar et al., 2005; Ellis et al., 2002; Schauble et al., 2004). Because V also has various valences in natural systems, remarkable fractionation of V isotopes is expected. Thus V isotope compositions of terrestrial samples may fingerprint redox-state variation.

It is important to understand how V isotopes are fractionated during processes controlling V transportation and deposition in the Earth's surface system, i.e., adsorption and redox reactions. To present, there has been no experimental work to investigate V isotope fractionation among V species with different valences and during mineral adsorption. With advancements in computational chemistry, equilibrium isotope fractionation factors can be obtained by first-principles calculations. Quantum chemistry calculations combined with the Urey model or Bigeleisen–Mayer equation (Bigeleisen and Mayer, 1947; Urey, 1947) can provide a reliable way to obtain isotope fractionation factors. This method has been successfully applied to calculate equilibrium isotope fractionation factors of many systems such as Fe, Cu, Zn, Cr, and Ge (e.g., Anbar et al., 2005; Fujii et al., 2014; Li et al., 2009; Schauble et al., 2004; Sherman, 2013).

In this study, V isotopic equilibrium fractionation factors of selected V species with valences +3, +4, or +5, including $[V^{5+}O_3(OH)]^{2-}$, $[V^{5+}O_2(H_2O)_4]^+$, $[V^{5+}O_2(OH)_2]^-$, $[V^{4+}O(H_2O)_5]^{2+}$, $[V^{4+}O(OH)_2(H_2O)_3]$, and $[V^{3+}(OH)_3(H_2O)_3]$ were calculated using density functional theory. Among these, $[V^{5+}O_3(OH)]^{2-}$ and

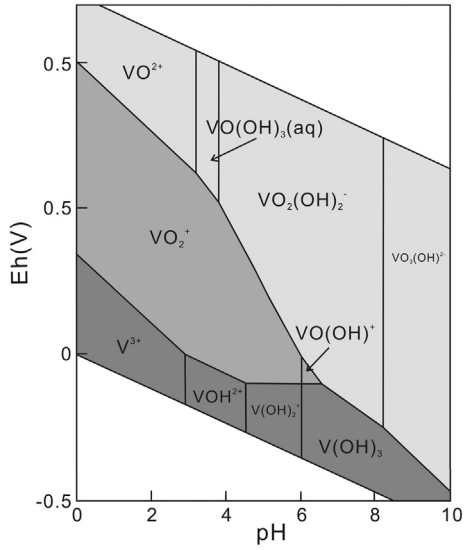

Fig. 1. Eh–pH diagram for vanadium aqueous species in the system V–O-H at 25 °C and 1 atm. $[V]_{total} < 2 \times 10^{-5}$ m (modified from Baes and Mesmer, 1976).

$[V^{5+}O_2(OH)_2]^-$ are dominant V(V) species in natural water under oxic conditions (Fig. 1). $[V^{5+}O_2(H_2O)_4]^+$ is the main form of V(V) in acid solution (pH < ~2, Fig. 1). $[V^{4+}O(H_2O)_5]^{2+}$, $[V^{4+}O(OH)_2(H_2O)_3]$, and $[V^{3+}(OH)_3(H_2O)_3]$ were investigated since they are among the common inorganic V(IV) and V(III) forms in solution under anoxic and euxinic conditions (Fig. 1). We also calculated the V isotope fractionation due to adsorption of V(V) species on the surface of goethite, since goethite, as a representative mineral adsorbent, is one of the most stable iron oxides and oxyhydroxide phases, and exists widely in chemical sediments and weathered soil (Langmuir et al., 1997). To reinforce the reliability of our results, we further calculated the V isotope fractionation factors of V^{4+}O-Lactate complex systems (VO(D-(−)-lact), VO(L-(+)-lact) and $[VO(lact)_2]^{2-}$), which could be compared with the chromatographic experimental results from Zhang et al. (2003). The purpose is to constrain V isotope fractionations caused by redox reaction in solution and adsorption on the mineral surface. This work provides a theoretical approach to employ V isotopes to investigate variations of redox conditions in paleo-ocean and paleo-atmosphere and to trace the source and transportation of anthropogenic V.

2. Methods

2.1. First-principles calculations

Mass dependent equilibrium isotope fractionation factors were calculated using the Urey model (Urey, 1947) or the Bigeleisen–Mayer equation (Bigeleisen and Mayer, 1947). The isotope fractionation factors are reported in the form of $10^3 \ln\alpha_{A-B}$ ($10^3 \ln\alpha_{A-B} = 10^3(\ln\beta_A - \ln\beta_B)$, where β_A and β_B represent the reduced partition function ratio of phase A and B, respectively). The reduced partition function ratio (β_A) of element X of phase A is calculated in a harmonic approximation, using the Teller–Redlich rule to simplify the calculation procedure (Redlich, 1935). The reduced partition function ratio depends on temperature and vibrational frequencies. The equation used to calculate the reduced partition function ratios is below:

$$\beta_A = \frac{Q^*}{Q} = \prod_i^{3N-6} \frac{\mu_i^*}{\mu_i} \frac{e^{-1/2\mu_i^*}}{(1-e^{-\mu_i^*})} \frac{(1-e^{-\mu_i})}{e^{-1/2\mu_i}} \quad (1)$$

where Q is the vibrational partition function, and * refers to the heavy isotope system. All the calculations were run over $3N-6$

vibrational modes for non-linear and polyatomic molecules consisting of N atoms. $\mu_i = h\nu_i/k_B T$, where h is the Plank constant, k_B is Boltzmann's constant, T is the temperature in Kevin, and ν_i represents the vibrational frequency of the ith mode.

The harmonic vibrational frequencies were computed by first principles calculations. In this study, all calculations, including geometry optimization and frequency calculations, were performed at the B3LYP/6-311+G(d,p) level (Lee et al., 1988) using Gaussian 03 package (Frisch et al., 2004). Previous studies have shown that this level can produce good accuracy with moderate computational cost (Fujii et al., 2014; Li et al., 2009; Li and Liu, 2010, 2011). The calculated infra-red frequencies attributed to the V–O stretching vibration of some V species are generally consistent with experimental results, as shown in Table A.2. Similar to some investigations of transitional element fractionation, such as Fe, Ni, Cu and Zn (Fujii et al., 2014), no scaling factors were used in the calculations.

2.2. Structures of V species and V(V) adsorption surface complexes

Structures of chosen V species in solution i.e., $[V^{5+}O_3(OH)]^{2-}$, $[V^{5+}O_2(H_2O)_4]^{+}$, $[V^{5+}O_2(OH)_2]^{-}$, $[V^{4+}O(H_2O)_5]^{2+}$, $[V^{4+}O(OH)_2(H_2O)_3]$, and $[V^{3+}(OH)_3(H_2O)_3]$, were modeled. Among the calculated species, $[V^{5+}O_3(OH)]^{2-}$ and $[V^{5+}O_2(OH)_2]^{-}$ occur in solutions with fourfold coordinated phosphate-like cluster structures (Rehder, 2008; Wehrli and Stumm, 1989); $[V^{5+}O_2(H_2O)_4]^{+}$, $[V^{4+}O(H_2O)_5]^{2+}$, $[V^{4+}O(OH)_2(H_2O)_3]$ and $[V^{3+}(OH)_3(H_2O)_3]$ show a sixfold coordination environment in solutions (Rehder, 2008). The V^{4+}O-Lactate complexes (VO(lact) and $[VO(lact)_2]^{2-}$) exhibit a structure of square pyramidal geometry.

A $[Fe_2(OH)_2(H_2O)_8]^{4+}$ dimer is conventionally used to represent the goethite surface structure (e.g., Peacock and Sherman, 2004a, 2004b). In addition, because a $[Fe_2(OH)_2(H_2O)_8]^{4+}$ dimer contains almost all the important surface sites of Fe(III) oxyhydroxides, it can also be used to represent the surface structure of Fe(III)-oxyhydroxides (e.g. Cornell and Schwertmann, 2006).

There are at least three possible structures of adsorption complexes on the surface of goethite, i.e. bidentate corner-sharing, bidentate edge-sharing surface complexes and monodentate surface complex. Among all the complexes, bidentate corner-sharing complexes mainly formed on the dominant surfaces of goethite (Boily et al., 2001). Furthermore, for V system, according to the structures determined by Peacock and Sherman (2004b) using both EXAFS spectroscopy and *ab-initio* calculations, the bidentate corner-sharing complexes (here expressed as $Fe_2O_2V(OH)_2^+$ and $Fe_2O_2VO(OH)$) are the most favorable configurations based on the energy level (see Fig. 7 of Peacock and Sherman, 2004b). Similar surface complexes are also found for Cu (Peacock and Sherman, 2004b) and U (Sherman et al., 2008) adsorbed onto the surface of goethite. Therefore the bidentate corner-sharing complexes were adopted in this study.

We simulated solvation effects by adopting the "water-droplet" method, in which the V-species are surrounded by explicit water molecules. In this study, we ran all the calculations (structure optimization and frequencies calculations) with all atoms free, similar to previous work (Li et al., 2009; Li and Liu, 2010, 2011; Liu and Tossell, 2005; Rustad et al., 2010). We initially put 6 water molecules around each V species, optimized the geometry, and then calculated the harmonic frequencies. After that, 6 additional water molecules were added to the previously optimized V-species with 6 water molecules, and optimization and frequencies calculations were repeated. These processes were iterated until the calculated $\ln\beta$ of V-species (with various number of water molecules) converged. For V(V) adsorption surface complexes, the same process was run with 3 water molecules each time.

Table 1
Calculated geometrical properties of vanadium species in this study, compared with literature values.

Formula	Bond type	Mean bond distances (Å)	
$[V^{3+}(OH)_3(H_2O)_3]$	V–O	2.06	This work
		2.01	Literature[a]
$[V^{4+}O(OH)_2(H_2O)_3]$	V=O	1.62	This work
	V–O(OH)	1.91	This work
	V–O(H_2O axial)	2.52	This work
	V–O(H_2O equatorial)	2.14	This work
$[V^{4+}O(H_2O)_5]^{2+}$	V=O	1.58	This work
		1.59	Literature[a]
	V–O(H_2O axial)	2.40	This work
		2.21	Literature[a]
	V–O(H_2O equatorial)	2.03	This work
		2.03	Literature[a]
$[V^{5+}O_2(OH)_2]^{-}$	V=O	1.64	This work
	V–O(OH)	1.80	This work
$[V^{5+}O_3(OH)]^{2-}$	V=O	1.68	This work
	V–O(OH)	1.87	This work
$[V^{5+}O_2(H_2O)_4]^{+}$	V=O	1.60	This work
		1.63	Literature[a]
	V–O(H_2O axial)	2.38	This work
		2.22	Literature[a]
	V–O(H_2O equatorial)	2.00	This work
		2.00	Literature[a]
$Fe_2O_2V(OH)_2^+$	V–O	1.76	This work
		1.67	Literature[b]
	V–Fe	3.11	This work
		3.25	Literature[b]
$Fe_2O_2VO(OH)$	V–O	1.74	This work
		1.67	Literature[b]
	V–Fe	3.22	This work
		3.23	Literature[b]

[a] Literature data is from EXAFS analysis results from Krakowiak et al. (2012).
[b] Literature data is from EXAFS analysis results from Peacock and Sherman (2004b).

3. Results

Optimized structures of all species are shown in Fig. 2 and V(V) adsorption surface complexes are shown in Fig. 3. Optimized structures of V^{4+}O-Lactate complexes are shown in Fig. A.1. The geometries and frequencies used in this paper are provided in Supplementary data (Appendix B). Comparison of calculated geometrical properties of surface complexes with literature values is shown in Table 1. The calculated structure of goethite surface agrees with previous studies (Li and Liu, 2011; Peacock and Sherman, 2004a, 2004b). The distance between the two Fe atoms is 3.0 Å and the mean bond length of four bridging Fe–O bonds is 1.89 Å. In the $Fe_2O_2V(OH)_2^+$ complexes (Fig. 3b), the mean bond lengths of V–O, Fe–Fe, and Fe–V are 1.76 Å, 2.90 Å, and 3.11 Å, respectively; and for the $Fe_2O_2VO(OH)$ complexes (Fig. 3c), the mean bond lengths of V–O, Fe–Fe and Fe–V, are 1.74 Å, 2.89 Å, and 3.22 Å, respectively.

We calculated $10^3\ln\beta$ for a series of water-droplet models with 6, 12, 18, and 24 water molecules for V species, and 3, 6, 9, and 12 water molecules for V(V) adsorption surface complexes that adsorb V(V). The reduced partition function ratio (β factor) calculated with water-droplet models can be affected by the numbers of surrounding water molecules. The relationship between $10^3\ln\beta$ of V species and the number of water molecules are presented in Fig. 4. As shown in Fig. 4, because the $10^3\ln\beta$ do not obviously change with more than 12 water molecules, adding 12 water molecules is sufficient to simulate the solvation effects for the V species. In order to reduce the possible error in calculation, the final $10^3\ln\beta$ of V species are taken from the averages of the water-droplets with 12, 18, and 24 water molecules. For the V(V) adsorption surface complexes, the preferred $10^3\ln\beta$ values come from the averages of models using 6, 9, and 12 water molecules. Considering the com-

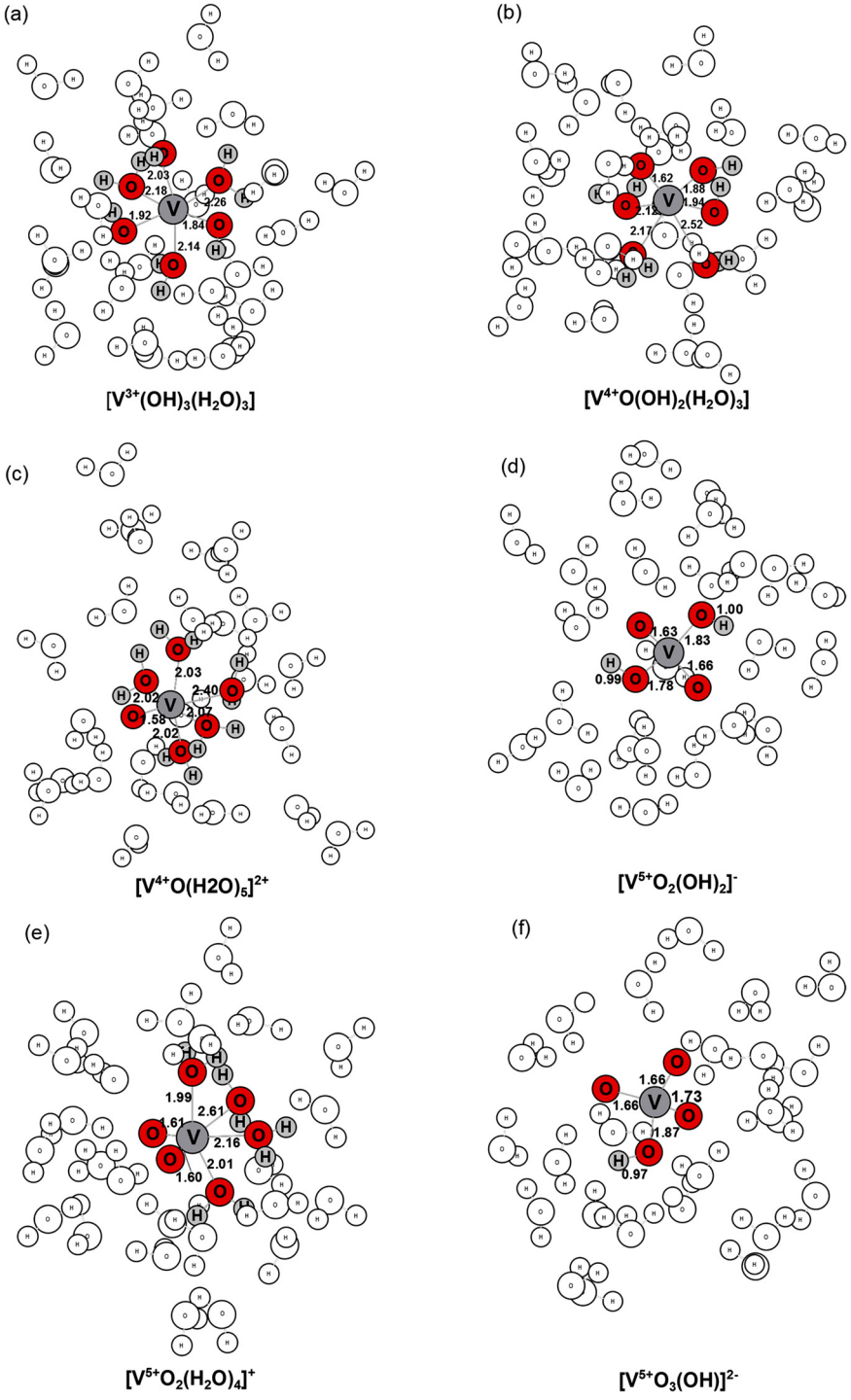

Fig. 2. Structures of vanadium cluster species with 24 water molecules: (a) $[V^{3+}(OH)_3(H_2O)_3]$, (b) $[V^{4+}O(OH)_2(H_2O)_3]$, (c) $[V^{4+}O(H_2O)_5]^{2+}$, (d) $[V^{5+}O_2(OH)_2]^-$, (e) $[V^{5+}O_2(H_2O)_4]^+$ and (f) $[V^{5+}O_3(OH)]^{2-}$. CN of V in $[V^{5+}O_2(OH)_2]^-$ (d) and $[V^{5+}O_3(OH)]^{2-}$ (f) is 4. In the other species (a, b, c and e), the CN of V is 6.

putational cost, we only report the $10^3 \ln\beta$ values of V^{4+}O-Lactate complexes with 6 water molecules added. This result is enough for us to test the reliability of our calculation. The standard deviations (SD) for our calculation of $\ln\beta$ on species at 25 °C range from 0.06‰ to 0.21‰ for $[V^{5+}O_3(OH)]^{2-}$ and $[V^{5+}O_2(H_2O)_4]^+$, which can be used to represent the accuracy of our calculations of $\ln\beta$.

The calculated $10^3 \ln\beta$ of V species versus temperature are showed in Fig. 5. Polynomial fitting factors of the $10^3 \ln\beta$ are presented in Table A.1. As shown in Fig. 5, the V isotopes are fractionated between different valence species. More specifically, the δ^{51}V enrichment order follows a sequence of $[V^{5+}O_2(OH)_2]^- \approx [V^{5+}O_3(OH)]^{2-} > [V^{5+}O_2(H_2O)_4]^+ > [V^{4+}O(OH)_2(H_2O)_3] \approx [V^{4+}O(H_2O)_5]^{2+} > [V^{3+}(OH)_3(H_2O)_3]$. The equilibrium isotopic fractionation factors between V(V) species and their surface complexes onto goethite are plotted in Fig. 6. V isotopes can be fractionated during the adsorption process with V(V) adsorption surface complexes enriching the ^{50}V relative to the corresponding V(V) species (Fig. 6). In addition, the equilibrium isotopic fractionation factors between $[V^{4+}O(H_2O)_5]^{2+}$ and V^{4+}O-Lactate complexes ($\ln\alpha_{V(IV)-V(IV)\text{-Lactate}}$) are −0.3 to −1‰ at 25 °C (Table A.1), comparable with previously published results from Zhang et al. (2003).

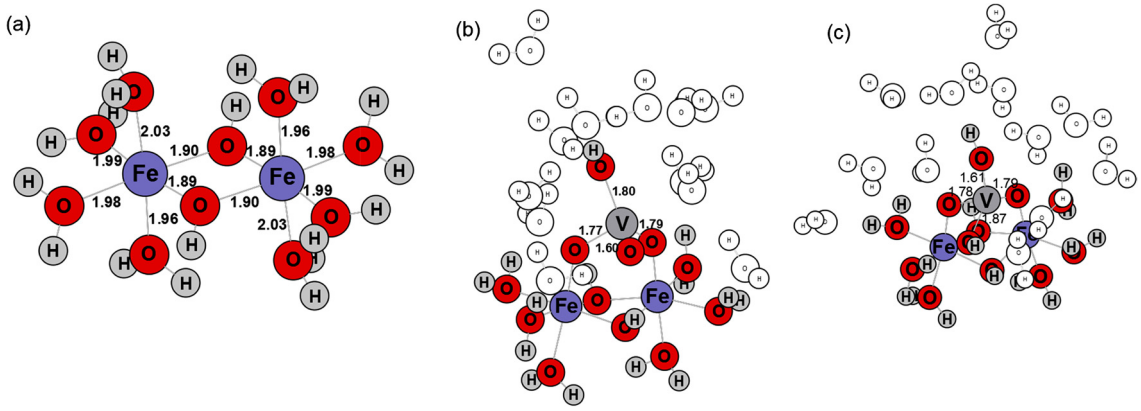

Fig. 3. Cluster models of (a) Fe(III) hydroxide dimer $[Fe_2(OH)_2(H_2O)_8]^{4+}$, and cluster with 12 water molecules of (b) $Fe_2O_2VO(OH)$ and (c) $Fe_2O_2V(OH)_2^+$.

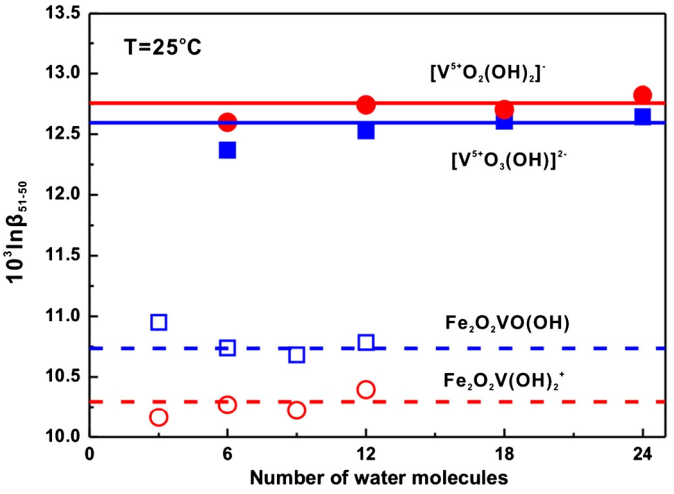

Fig. 4. $10^3 \ln\beta$ vs. the number of water molecules for $[V^{5+}O_2(OH)_2]^-$ and $[V^{5+}O_3(OH)]^{2-}$, and the adsorption surface complexes ($Fe_2O_2VO(OH)$ and $Fe_2O_2V(OH)_2^+$) at 25 °C.

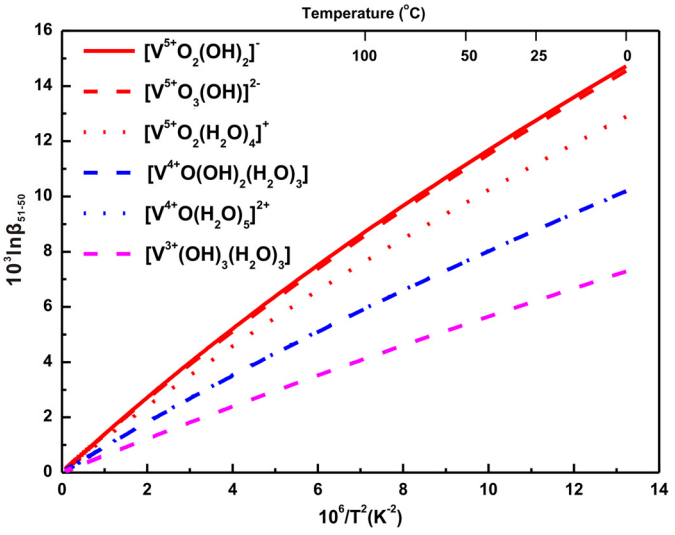

Fig. 5. The temperature dependence of reduced partition function ratios ($10^3 \ln\beta_{51-50}$) for V species with different valence states.

4. Controlling factors of equilibrium fractionation of vanadium clusters

Equilibrium isotope fractionation is controlled by bond strength (e.g., Bigeleisen and Mayer, 1947; Urey, 1947). Previous work showed that species with shorter chemical bonds tend to be enriched in heavy isotopes relative to species with longer chemical bonds, as they have stronger bond strength with higher vibrational frequency (e.g., Hill and Schauble, 2008; Schauble et al., 2004; Urey, 1947). In this study, there is also a negative correlation between $10^3 \ln\beta_{51-50}$ of V isotope and average V–O bond length in V species as showed in Fig. 7, in line with the general theory of equilibrium isotope fractionation.

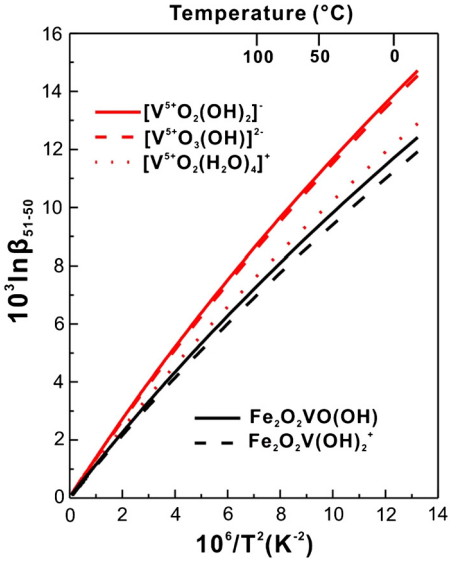

Fig. 6. The temperature dependence of $10^3 \ln\beta_{51-50}$ for V(V) species ($[V^{5+}O_2(OH)_2]^-$, $[V^{5+}O_3(OH)]^{2-}$ and $[V^{4+}O(H_2O)_5]^{2+}$) and the V(V) adsorption surface complexes of goethite ($Fe_2O_2VO(OH)$ and $Fe_2O_2V(OH)_2^+$).

The oxidation state of V is the major factor to influence isotope fractionation among different species. As shown in Fig. 5, V species with high valence state tend to be enriched in ^{51}V. For example, at 25 °C, the equilibrium fractionation factor between V(V) and V(IV) species ($\ln\alpha_{V(V)-V(IV)}$) varies from 2.34 to 3.92‰. Similar phenomena are also documented for other redox sensitive elements, like Cu (Sherman, 2013), Cr (Schauble et al., 2004), and Fe (Anbar et al., 2005). From the structural perspective, V–O bond length (particularly for the same bond types) decreases and bond strength increases with increasing valence state. As shown in Fig. 7, V species with higher valance state show a shorter average V–O bond and are enriched in heavier isotopes.

Isotope fractionation also occurs among species with different CN. Fig. 5 shows that $[V^{5+}O_2(OH)_2]^-$ and $[V^{5+}O_3(OH)]^{2-}$, existing as 4-fold coordinated clusters, are enriched in ^{51}V compared to 6-fold coordinated cluster $[V^{5+}O_2(H_2O)_4]^+$. Further, the difference of bond length and isotopic fractionation is negligible between

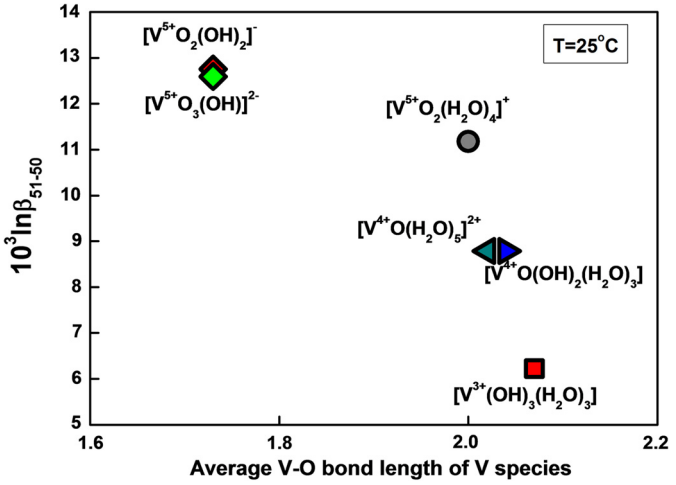

Fig. 7. The negative correlation between $10^3 \ln\beta_{51-50}$ for V species and average V–O bond length at 25 °C. V species with high valence state show shorter V–O bond length and higher $10^3 \ln\beta_{51-50}$. V(V) species with different CN also show different V–O bond length. $[V^{5+}O_2(OH)_2]^-$ and $[V^{(5+}O_3(OH)]^{2-}$ with four-fold CN have shorter V–O bond length than $[V^{5+}O_2(H_2O)_4]^+$ with six-fold CN.

$[V^{4+}O(H_2O)_5]^{2+}$ and $[V^{4+}O(OH)_2(H_2O)_3]$, which are both 6-fold coordinated V species with the same +4 valence.

The clusters of V(V)-goethite surface complexes ($Fe_2O_2V(OH)_2^+$ and $Fe_2O_2VO(OH)$) are enriched in ^{50}V compared to the V(V) clusters in solution despite the similarity of their average bond length of V–O (Fig. 7), perhaps as a result of distortion in V(V)-goethite complexes. Our calculations showed that the structures of adsorbed V species are distorted by forming the bidentate corner-sharing complexes. For instance, all the O–V–O bond angles are near 110° for $[V^{5+}O_3(OH)]^{2-}$, while the (Fe–)O–V–O(–Fe) bond angle is 85° for $Fe_2O_2VO(OH)$. The distortion of the adsorption surface complexes should decrease the stability and bond strength of V–O bonds in the first coordination sphere, and cause enrichment of ^{50}V in the adsorption surface complexes. Similar mechanisms have also been used to explain the isotope fractionation during surface adsorption processes of Ge (Pokrovsky et al., 2014) and Mo (Barling and Anbar, 2004).

5. Geological applications

5.1. Implications for monitoring environmentally toxic V(V)

As a contaminant in water, most waste V is generated by the ferrous metallurgy industry (World Health Organization, 1988). To reduce the potential risk of this toxic element, it is important to monitor the attenuation of V in water. Because V is a highly redox-active element, its mobility and environmental impact in water mainly depend on redox reaction and adsorption processes. Our calculations predicts large fractionation of V isotopes among species of different valences and during V(V) adsorption on goethite. Thus, V isotope data could be used to trace toxic V(V) transportation and removal processes in solution.

To quantify isotopic shifts of V in solutions during removal processes, we developed a numerical model simulating isotope fractionation in a closed system by batch or Rayleigh fractionation. This approach has been widely used in the literature to explain isotopic fractionation of Se, Fe, Cr, and U during redox reactions (e.g., Ellis et al., 2002; Johnson and Bullen, 2004). In such models, the isotope fractionation factor (α) is conventionally defined as

$$\alpha = R_{\text{products}}/R_{\text{reactants}} \tag{2}$$

where R_{products} refers to the $^{51}V/^{50}V$ of the V reduced or adsorbed during the reaction in a closed system fractionation or at an instant in time for Rayleigh fractionation, and $R_{\text{reactants}}$ refers to the $^{51}V/^{50}V$ ratios of the V remaining in the reactant pool. Then in a closed system, the V isotope composition of remaining unreacted V(V) in solution ($\delta^{51}V$) can be described as:

$$\delta^{51}V = (\delta^{51}V_{\text{initial}} + 10^3) \times [(f-1) \times \ln\alpha + 1] - 10^3 \tag{3}$$

In an open system that can be described as a Rayleigh fractionation process, $\delta^{51}V$ could be described as equation (4):

$$\delta^{51}V = [(\delta^{51}V_{\text{initial}} + 10^3) \times (\ln f^{(\alpha-1)} + 1)] - 10^3 \tag{4}$$

In equations (3) and (4), $\delta^{51}V_{\text{initial}}$ refers to the V isotopic composition of the initial solution, and f is the fraction of residual unreacted V(V).

Assuming that isotopic exchange equilibrium between V(V) species and other V species is reached, the isotope fractionation factor during reduction reaction and adsorption could be estimated based on equilibrium isotopic fractionation among different V species. V(V) would form polynuclear species in V contaminated water at high concentration of V(V), and the V isotopic composition of polynuclear species might be different from mononuclear species. However, such species only exist as the primary V(V) species at concentrations in excess of ~1 mmol/L (Rehder, 2008), which is higher than that of most natural solutions even at environmentally-impacted sites. Therefore, vanadate ($[V^{5+}O_3(OH)]^{2-}$ and $[V^{5+}O_2(OH)_2]^-$) is chosen to represent V(V) species here, since they are supposed to be the dominant V(V) species in most natural solutions as shown in Fig. 1. Meanwhile, $[V^{4+}O(H_2O)_5]^{2+}$, $[V^{4+}O(OH)_2(H_2O)_3]$, and $[V^{3+}(OH)_3(H_2O)_3]$ are tentatively assumed to represent the V(IV) and V(III) species respectively in the current study. Based on such assumptions, we can model the variation of $\delta^{51}V$ of residual V(V) dissolved in the solution during such redox and adsorption processes (Fig. 8).

Our model indicates that as V(V) content decreases due to reduction or adsorption, ^{51}V is preferentially enriched in V(V) species. $\delta^{51}V$ of the remaining V(V) could increase by several ‰, very large change relative to the precision of the present analysis (0.12–0.15‰ 2SD, Prytulak et al., 2011; Nielsen et al., 2011) (Fig. 8). Since $\delta^{51}V$ variations in solution are strongly related to the extent of reduction or adsorption, V isotope ratios can be used as indicators of the extent of V(V) attenuation in natural solution.

5.2. Oceanic V isotope budget and its geological implication

Understanding of the oceanic V flux and isotope mass balance is the key to developing V isotope geochemistry as a new paleo-redox proxy. Our calculation can provide theoretical predictions of V isotope budget for the ocean. The geochemical cycle of V in the oceans is mainly controlled by environmental redox conditions because the change of redox state can influence the flux proportions of V outputs from the ocean (e.g., Morford and Emerson, 1999; Algeo and Maynard, 2004). The oceanic cycle of an element can be evaluated based on the elemental flux mass balance (e.g., Tipper et al., 2006). In general, the V inputs to the ocean are equal to the outputs from the ocean at the steady state:

$$F_{\text{in}} = F_{\text{out}} \tag{5}$$

where F_{in} is the input flux and F_{out} is the output flux of the ocean. River input is considered as the main source of V to the ocean, and the main output from the ocean is marine sediments in oxic-reduced environments and hydrothermal deposits (see Morford and Emerson, 1999 and references therein). Assuming no output other than these three sinks, equation (5) can further be expressed as:

$$F_R = F_O + F_A + F_H \tag{6}$$

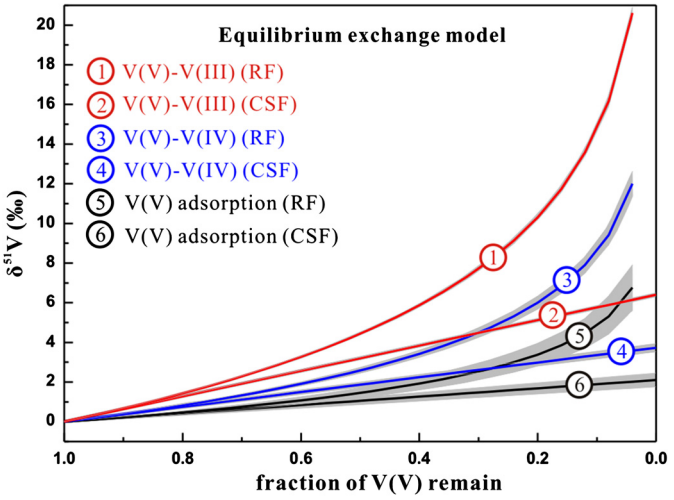

Fig. 8. Isotope equilibrium exchange model for δ^{51}V of remaining unreacted V(V) versus the fraction of residual unreacted V(V) in the solution. In this model, we define $\alpha_{V(IV)-V(V)} = 0.9963 \pm 0.0002$, $\alpha_{V(III)-V(V)} = 0.9936 \pm 0.0001$, $\alpha_{V(V)adsorbed-V(V)} = 0.9979 \pm 0.0004$ and assume $\delta^{51}V_{initial} = 0$ (see detailed discussion in the texts). Red lines: V(V) reduced to V(III). Blue lines: V(V) reduced to V(IV). Black lines: V(V) adsorbed by goethite. The lightly shaded areas represent the range of our models for each equilibrium exchange reaction. Abbreviations: RF, Rayleigh fractionation model; CSF, closed system fractionation model. (For interpretation of the references to color in this figure legend, the reader is referred to the web version of this article.)

In equation (6), F_R represents river flux into the ocean as the main V input, F_O represents flux of the oxic sink where V(V) is adsorbed by Fe–Mn oxide and deposited in oxic conditions, F_A represents the flux of the reduced sink (both anoxic and euxinic) in which V with main valence of +4 or possibly +3 is removed from water lacking free oxygen, and F_H represents the flux due to hydrothermal precipitation of V (Breit and Wanty, 1991; Morford and Emerson, 1999 and references therein).

The V isotope budget of seawater creates additional constraints on oceanic V mass balance. Attempts were previously made to investigate oceanic mass balance of elements such as Mg (e.g., Tipper et al., 2006), Cu, and Zn (e.g., Little et al., 2014). Based on the steady-state model of the ocean, which presumes a balance between the influx from the continents and outflux into sediments, we get the equation:

$$\delta_{in} = f_O \times \delta_O + f_A \times \delta_A + f_H \times \delta_H \quad (7)$$

where δ refers to the V isotope composition of the different source and sinks, $f_x = (F_x/F_{in})$ refers to the fraction of V removed by these sinks. In additions, we get

$$f_O + f_A + f_H = 1 \quad (8)$$

from equation (6). Considering the V isotope fractionation between seawater and different sinks (i.e., $\Delta_{SW-X}{}^{51}V = \delta_{SW} - \delta_O$, where δ_{SW} refers to the V isotope composition of seawater), we further obtain the equation:

$$\delta_{SW} = \delta_{in} + f_O \times \Delta_{SW-O}{}^{51}V + f_A \times \Delta_{SW-A}{}^{51}V + f_H \times \Delta_{SW-H}{}^{51}V, \quad (9)$$

where δ_{SW} is the V isotope composition of seawater. Equation (9) reveals that seawater V isotope composition (δ_{SW}) is controlled by the V isotopic composition of input (δ_{in}) as well as the fraction of V removed into different sinks (f_X). Additionally, V isotope fractionation factors between seawater and different sinks are the key parameters to quantify the ocean V isotope mass balance. Here we use our calculation results to give a theoretical estimation of the ocean V isotope budget:

In the oxic environment of the ocean, the dominant species of V is vanadate (HVO_4^{2-} and $H_2VO_4^-$, see Fig. 1) with +5 valence. Vanadate is mainly scavenged by Fe and Mn oxides through an adsorption process in which sediments and ferromanganese nodules/crusts deposit under oxic conditions. Since goethite is one of main mineral that adsorb V(V), and sequential leaching experiments imply that V(V) species tend to be accumulated in ferromanganese nodules and crusts in the ocean through adsorption to goethite (Koschinsky and Hein, 2003), it is reasonable to assume that $\Delta^{51}V_{SW-O} \approx \Delta^{51}V_{V(V)\text{-goethite}}$. In addition, previous works on other metal stable isotope like Mo (e.g. Barling and Anbar, 2004) imply that adsorption process of transitional metal isotopes could be simulated as equilibrium isotope exchange reactions. Therefore, isotope fractionation factors of V between seawater and oxic sinks could be estimated using our model, i.e. $\Delta^{51}V_{SW-O} \approx \Delta^{51}V_{V(V)\text{-goethite}} = 2.1 \pm 0.4‰$.

Furthermore, in the modern oxic ocean, iron oxyhydroxide particles forming in hydrothermal systems by oxidation reactions can take up ocean V(V) through adsorption processes (Trefry and Metz, 1989). Assuming that goethite can represent iron oxides and oxyhydroxides for adsorption processes, as they show similar surface structures (e.g. Cornell and Schwertmann, 2006), the V isotopic composition of hydrothermal systems could also be approximately expressed as $\Delta^{51}V_{SW-H} \approx \Delta^{51}V_{V(V)\text{-goethite}} = 2.1 \pm 0.4‰$.

Under reducing conditions, V(V) is reduced to V(VI) or further to V(III), and such species are easily taken up by the sediment from seawater. The isotopic offset of V during accumulation into reduced sediment from seawater depends on both the proportion of V removed from the reactive pool and isotope fractionation of V during the reduction reaction. If the sequestration of V from seawater is quantitative, which is most likely the case given the ocean's pervasive lack of free oxygen, the isotopic composition of authigenic V in the reducing sediments is likely the same as that of the contemporaneous seawater, i.e. $\Delta_{SW-A}{}^{51}V \approx 0$. Otherwise, if V(V) is partially reduced and taken up from the water, isotope fractionation of V during the reduction reaction is the key parameter to control Δ_{SW-A}. Stratified water columns in which anoxic water underlies oxic water favor such partial reduction. In addition, assuming isotope exchange for V is fast enough so that isotopic equilibration is reached during the reduction reaction of V(V), we can give a rough estimation of Δ_{SW-A} based on our calculation, i.e. $\Delta_{SW-A}{}^{51}V \approx 3.7 \sim 6.4‰$.

Combining our estimation of $\Delta_{SW-X}{}^{51}V$ with equation (8) and (9), we plotted the variations of V isotope offset between the dissolved V of seawater and the global input ($\delta_{SW} - \delta_{in}$) along with the change of f_A (Fig. 9). In Fig. 9, both the quantitative V sequestration model with $\Delta_{SW-A}{}^{51}V = 0$ (Model 1 in Fig. 9) and V isotope equilibration model with $\Delta_{SW-A}{}^{51}V = 3.7$–$6.4‰$ (Model 2 in Fig. 9) are simulated. The vertical shaded area shows the estimated modern value of the proportion of riverine flux removed from anoxic sediment ($8 \pm 5\%$, Emerson and Huested, 1991). Although the exact V isotope offset of different sinks from seawater inventory cannot be obtained with any accuracy, our calculations support the idea that changes of oceanic redox conditions influence $\delta^{51}V_{SW}$ via changes of the relative proportions of different sinks, as shown in Fig. 9. In addition, such variations of $\delta^{51}V_{SW}$ are likely to be recorded in the oceanic sediments. Thus, although there is currently no V isotope measurement for seawater and ocean sediment, our theoretical work provides basic parameters to constrain V isotope fractionation between ocean inventory and different sinks, implying that $\delta^{51}V$ records of ancient sedimentary rocks may offer insights into regional or global redox conditions of the paleo-ocean.

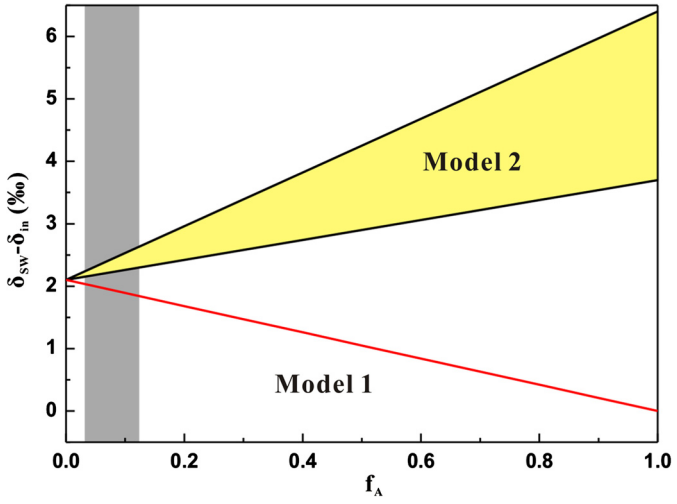

Fig. 9. Models for the shift of $\delta^{51}V$ between seawater reservoir and river inputs ($\delta_{SW}-\delta_{in}$) versus proportion of riverine flux removed by anoxic sink (f_A). Two possible models of isotope shift with different assumed V isotope fractionation factors between seawater and reducing sinks are presented. In model 1, $\Delta_{SW\text{-}O}{}^{51}V = 2.1‰$, $\Delta_{SW\text{-}H}{}^{51}V = 2.1‰$, and $\Delta_{SW\text{-}A}{}^{51}V = 0$. In model 2, $\Delta_{SW\text{-}O}{}^{51}V = 2.1‰$, $\Delta_{SW\text{-}H}{}^{51}V = 2.1‰$, and $\Delta_{SW\text{-}A}{}^{51}V = 3.7\text{–}6.4‰$. The vertical shaded area shows the estimated modern value of proportion of riverine flux removed from anoxic sediment. See detailed discussions in the text.

6. Conclusions

Equilibrium V isotope fractionation factors among dominant V species of different valences in solution and V(V)-goethite surface complexes were calculated using first-principles calculations. Our calculations predict significant V isotope fractionation among V species with different valences, following a general trend of enrichment of ^{51}V isotopes as $VO_2(OH)_2^- \approx VO_3(OH)^{2-} > VO_2(H_2O)_4^+ > VO(OH)_2(H_2O)_3 \approx VO(H_2O)_5^{2+} > V(OH)_3(H_2O)_3$. Our results also reveal that ^{50}V is preferentially adsorbed onto the surface of goethite during adsorption of V(V) species. Our theoretical estimation predicts that large V isotope fractionation could occur during V transportation and segregation in natural solutions via redox reaction and adsorption processes. A rough estimation of oceanic V isotope mass balance is also presented based on our calculation. This work implies that V isotope fractionation is promising as a potential paleo-redox tracer and an indicator to monitor the attenuation of V(V) in polluted systems.

Acknowledgements

This work is supported by State Key Development Program of Basic Research of China (2014CB845905), the National Natural Science Foundation of China (41173031, 41473011, and 41090370), the Chinese Academy of Sciences International Partnership Program for Creative Research Teams to Z.Q. Wu, the 111 project and the Fundamental Research Funds for the Central Universities for F. Huang. We thank Derek Vance for comments and editorial handling. We are also grateful to Sune G. Nielsen and two anonymous reviewers for constructive comments which significantly improve the manuscript. The computations were partially conducted in Shanghai supercomputer center. We are also grateful to Ed Schauble for helpful discussion.

Appendix. Supplementary material

Supplementary material related to this article can be found online at http://dx.doi.org/10.1016/j.epsl.2015.06.048.

References

Algeo, T.J., Maynard, J.B., 2004. Trace-element behavior and redox facies in core shales of Upper Pennsylvanian Kansas-type cyclothems. Chem. Geol. 206, 289–318.
Anbar, A.D., Jarzecki, A.A., Spiro, T.G., 2005. Theoretical investigation of iron isotope fractionation between $Fe(H_2O)_6^{3+}$ and $Fe(H_2O)_6^{2+}$: implications for iron stable isotope geochemistry. Geochim. Cosmochim. Acta 69, 825–837.
Auger, Y., Bodineau, L., Leclercq, S., Wartel, M., 1999. Some aspects of vanadium and chromium chemistry in the English Channel. Cont. Shelf Res. 19, 2003–2018.
Baes, C.F., Mesmer, R.E., 1976. Hydrolysis of Cations. Wiley.
Barling, J., Anbar, A.D., 2004. Molybdenum isotope fractionation during adsorption by manganese oxides. Earth Planet. Sci. Lett. 217, 315–329.
Bigeleisen, J., Mayer, M.G., 1947. Calculation of equilibrium constants for isotopic exchange reactions. J. Chem. Phys. 15, 261–267.
Boily, J.-F., Lützenkirchen, J., Balmès, O., Beattie, J., Sjöberg, S., 2001. Modeling proton binding at the goethite (α-FeOOH)–water interface. Colloids Surf. A, Physicochem. Eng. Asp. 179, 11–27.
Breit, G.N., 1995. Origin of clay minerals associated with V–U deposits in the Entrada Sandstone, Placerville mining district, southwestern Colorado. Econ. Geol. 90, 407–419.
Breit, G.N., Wanty, R.B., 1991. Vanadium accumulation in carbonaceous rocks – a review of geochemical controls during deposition and diagenesis. Chem. Geol. 91, 83–97.
Cornell, R.M., Schwertmann, U., 2006. The Iron Oxides: Structure, Properties, Reactions, Occurrences and Uses. John Wiley & Sons.
Elderfield, H., Schultz, A., 1996. Mid-ocean ridge hydrothermal fluxes and the chemical composition of the ocean. Annu. Rev. Earth Planet. Sci. 24, 191–224.
Ellis, A.S., Johnson, T.M., Bullen, T.D., 2002. Chromium isotopes and the fate of hexavalent chromium in the environment. Science 295, 2060–2062.
Emerson, S.R., Huested, S.S., 1991. Ocean anoxia and the concentrations of molybdenum and vanadium in seawater. Mar. Chem. 34, 177–196.
Frisch, M., Trucks, G., Schlegel, H., Scuseria, G., Robb, M., Cheeseman, J., Montgomery Jr., J., Vreven, T., Kudin, K., Burant, J., 2004. Gaussian 03, revision c. 02, Gaussian. Inc., Wallingford, CT.
Fujii, T., Moynier, F., Blichert-Toft, J., Albarède, F., 2014. Density functional theory estimation of isotope fractionation of Fe, Ni, Cu, and Zn among species relevant to geochemical and biological environments. Geochim. Cosmochim. Acta 140, 553–576.
Hill, P.S., Schauble, E.A., 2008. Modeling the effects of bond environment on equilibrium iron isotope fractionation in ferric aquo–chloro complexes. Geochim. Cosmochim. Acta 72, 1939–1958.
Johnson, T.M., Bullen, T.D., 2004. Mass-dependent fractionation of selenium and chromium isotopes in low-temperature environments. Rev. Mineral. Geochem. 55, 289–317.
Koschinsky, A., Hein, J.R., 2003. Uptake of elements from seawater by ferromanganese crusts: solid-phase associations and seawater speciation. Mar. Geol. 198, 331–351.
Krakowiak, J., Lundberg, D., Persson, I., 2012. A coordination chemistry study of hydrated and solvated cationic vanadium ions in oxidation states +III, +IV, and +V in solution and solid state. Inorg. Chem. 51, 9598–9609.
Langmuir, D., Hall, P., Drever, J., 1997. Environmental Geochemistry. Prentice Hall, New Jersey.
Lee, C., Yang, W., Parr, R.G., 1988. Development of the Colle–Salvetti correlation-energy formula into a functional of the electron density. Phys. Rev. B 37, 785.
Lee, C.-T.A., Leeman, W.P., Canil, D., Li, Z.-X.A., 2005. Similar V/Sc systematics in MORB and arc basalts: implications for the oxygen fugacities of their mantle source regions. J. Petrol. 46, 2313–2336.
Li, X., Liu, Y., 2011. Equilibrium Se isotope fractionation parameters: a first-principles study. Earth Planet. Sci. Lett. 304, 113–120.
Li, X., Zhao, H., Tang, M., Liu, Y., 2009. Theoretical prediction for several important equilibrium Ge isotope fractionation factors and geological implications. Earth Planet. Sci. Lett. 287, 1–11.
Li, X.F., Liu, Y., 2010. First-principles study of Ge isotope fractionation during adsorption onto Fe(III)-oxyhydroxide surfaces. Chem. Geol. 278, 15–22.
Little, S.H., Vance, D., Walker-Brown, C., Landing, W.M., 2014. The oceanic mass balance of copper and zinc isotopes, investigated by analysis of their inputs, and outputs to ferromanganese oxide sediments. Geochim. Cosmochim. Acta 125, 673–693.
Liu, Y., Tossell, J.A., 2005. Ab initio molecular orbital calculations for boron isotope fractionations on boric acids and borates. Geochim. Cosmochim. Acta 69, 3995–4006.
McCrindle, C.M.E., Mokantla, E., Duncan, N., 2001. Peracute vanadium toxicity in cattle grazing near a vanadium mine. J. Environ. Monit. 3, 580–582.
Morford, J.L., Emerson, S., 1999. The geochemistry of redox sensitive trace metals in sediments. Geochim. Cosmochim. Acta 63, 1735–1750.
Nielsen, S.G., Prytulak, J., Halliday, A.N., 2011. Determination of precise and accurate $^{51}V/^{50}V$ isotope ratios by MC-ICP-MS, part 1: chemical separation of vanadium and mass spectrometric protocols. Geostand. Geoanal. Res. 35, 293–306.

Nielsen, S.G., Prytulak, J., Wood, B.J., Halliday, A.N., 2014. Vanadium isotopic difference between the silicate Earth and meteorites. Earth Planet. Sci. Lett. 389, 167–175.

Peacock, C.L., Sherman, D.M., 2004a. Copper (II) sorption onto goethite, hematite and lepidocrocite: a surface complexation model based on ab initio molecular geometries and EXAFS spectroscopy. Geochim. Cosmochim. Acta 68, 2623–2637.

Peacock, C.L., Sherman, D.M., 2004b. Vanadium(V) adsorption onto goethite (α-FeOOH) at pH 1.5 to 12: a surface complexation model based on ab initio molecular geometries and EXAFS spectroscopy. Geochim. Cosmochim. Acta 68, 1723–1733.

Pokrovsky, O.S., Galy, A., Schott, J., Pokrovski, G.S., Mantoura, S., 2014. Germanium isotope fractionation during Ge adsorption on goethite and its coprecipitation with Fe oxy(hydr)oxides. Geochim. Cosmochim. Acta 131, 138–149.

Prytulak, J., Nielsen, S.G., Halliday, A.N., 2011. Determination of precise and accurate $^{51}V/^{50}V$ isotope ratios by multi-collector ICP-MS, part 2: isotopic composition of six reference materials plus the Allende chondrite and verification tests. Geostand. Geoanal. Res. 35, 307–318.

Prytulak, J., Nielsen, S.G., Ionov, D.A., Halliday, A.N., Harvey, J., Kelley, K.A., Niu, Y.L., Peate, D.W., Shimizu, K., Sims, K.W.W., 2013. The stable vanadium isotope composition of the mantle and mafic lavas. Earth Planet. Sci. Lett. 365, 177–189.

Redlich, O., 1935. A general relationship between the oscillation frequency of isotropic molecules (with remarks on the calculation of harmonious force constants). Z. Phys. Chem., B Chem. Elem.proz. Aufbau Mater. 28, 371–382.

Rehder, D., 2008. Bioinorganic Vanadium Chemistry. John Wiley & Sons.

Rustad, J.R., Casey, W.H., Yin, Q.-Z., Bylaska, E.J., Felmy, A.R., Bogatko, S.A., Jackson, V.E., Dixon, D.A., 2010. Isotopic fractionation of $Mg^{2+}_{(aq)}$, $Ca^{2+}_{(aq)}$, and $Fe^{2+}_{(aq)}$ with carbonate minerals. Geochim. Cosmochim. Acta 74, 6301–6323.

Schauble, E., Rossman, G.R., Taylor Jr., H.P., 2004. Theoretical estimates of equilibrium chromium-isotope fractionations. Chem. Geol. 205, 99–114.

Sherman, D.M., 2013. Equilibrium isotopic fractionation of copper during oxidation/reduction, aqueous complexation and ore-forming processes: predictions from hybrid density functional theory. Geochim. Cosmochim. Acta 118, 85–97.

Sherman, D.M., Peacock, C.L., Hubbard, C.G., 2008. Surface complexation of U (VI) on goethite (α-FeOOH). Geochim. Cosmochim. Acta 72, 298–310.

Siebert, J., Badro, J., Antonangeli, D., Ryerson, F.J., 2013. Terrestrial accretion under oxidizing conditions. Science 339 (6124), 1194–1197.

Tipper, E.T., Galy, A., Gaillardet, J., Bickle, M.J., Elderfield, H., Carder, E.A., 2006. The magnesium isotope budget of the modern ocean: constraints from riverine magnesium isotope ratios. Earth Planet. Sci. Lett. 250, 241–253.

Trefry, J.H., Metz, S., 1989. Role of hydrothermal precipitates in the geochemical cycling of vanadium. Nature 342, 531–533.

Urey, H.C., 1947. The thermodynamic properties of isotopic substances. J. Chem. Soc. (Resumed), 562–581.

Wanty, R.B., Goldhaber, M.B., 1992. Thermodynamics and kinetics of reactions involving vanadium in natural systems: accumulation of vanadium in sedimentary rocks. Geochim. Cosmochim. Acta 56, 1471–1483.

Wehrli, B., Stumm, W., 1989. Vanadyl in natural waters: adsorption and hydrolysis promote oxygenation. Geochim. Cosmochim. Acta 53, 69–77.

World Health Organization, 1988. Environmental Health Criteria 81: Vanadium. WHO, Geneva.

Zhang, Y.-H., Nomura, M., Aida, M., Fujii, Y., 2003. Separation of vanadium isotopes by ion-exchange chromatography. J. Chromatogr. A 989, 175–182.